BMC Genomics

RESEARCH

Open Access

From unipotency to pluripotency: deciphering protein networks and signaling pathways in the generation of embryonic stem-like cells from murine spermatogonial stem cells

Nima Ghasemi[1], Hossein Azizi[2*], Ali Qorbanee[3] and Thomas Skutella[4]

Abstract

With the significant challenges in using human embryonic stem cells (ESCs) for research and clinical applications, there is a growing impetus to seek alternative pluripotent cell sources. Embryonic stem-like (ES-like) cells emerge as a promising avenue in this pursuit. Our research demonstrates the potential for deriving ES-like cells from spermatogonial stem cells (SSCs) in a time-dependent manner under defined culture conditions. To better understand this process, we investigated the gene expression dynamics and underlying pathways associated with ES-like cell generation from SSCs. A deeper understanding of the signaling pathways underlying this biological process can lead us to refine protocols for ES-like cell generation, which could catalyze the development of more efficient and expedited methodologies inspired by the derivation pathway for future research in regenerative medicine. To identify differentially expressed genes (DEGs), we analyzed publicly available microarray data from murine cells obtained from the Gene Expression Omnibus (GEO). This analysis enabled the prediction of protein–protein interactions (PPIs), which were subsequently used for pathway enrichment analysis to identify biologically relevant pathways. Complementing these computational findings, we conducted in vitro experiments, including Fluidigm qPCR and immunostaining. These experiments serve as validation for our microarray data and the DEGs identified, providing reassurance about the reliability of our research. Among the identified enriched pathways in our investigation are the Toll-like receptor (TLR), GDNF/RET, interleukins (ILs), FGF/FGFR, and SMAD signaling pathway, along with the activation of NIMA kinases. Additionally, miR-410-3p, miRNA let-7e, Miat, and Xist are among some of the predicted non-coding RNAs.

Keywords Spermatogonial stem cells, Embryonic stem-like cells, Microarray analysis, PPI network, Signaling pathways, miRNA and lncRNA

*Correspondence:
Hossein Azizi
h.azizi@ausmt.ac.ir
Full list of author information is available at the end of the article

Introduction

Mouse embryonic stem cells (mESCs) are pluripotent stem cells derived from the inner cell mass (ICM) of pre-implantation blastocysts, typically between embryonic day 3.5 and E.5 post-fertilization. They have many research and medical applications. ESCs have the extraordinary ability to divide and differentiate into all three germ layers. Their capabilities make them very promising candidates for various clinical applications, including cardiac diseases [1], eye diseases [2], wound healing [3], healing spinal cord injury (SCI) [4], and treating Alzheimer's disease (AD) [5]. Although ESCs hold immense potential for proliferation and differentiation across various cell types and tissues, their application remains constrained by several critical factors. Chief among these barriers are ethical concerns surrounding their extraction from human embryonic tissues [6]. Moreover, the complexity of the culture medium, especially the challenge of ensuring a Xenobiotics-free environment, as well as concerns about chromosome and genetic instability, and the immune rejection potential of ESCs-derived cells, serve as additional concerns in the use of ESCs, particularly in therapeutic applications [7].

Confronted with these obstacles in using ESCs, a new research trend emerged focused on generating pluripotent stem cells to facilitate progress in medicine. It didn't take long for nuclear reprogramming strategies to emerge, including methods such as somatic cell fusion with ESCs cells, which can induce a pluripotent state in specialized cells in addition to somatic cell nuclear transfer (SCNT), which has enabled the generation of cloned animals [8, 9]. Subsequently, it became apparent that by introducing Oct4, Sox2, Klf4, and c-Myc (OSKM) factors into adult fibroblasts, these somatic cells could be reprogrammed into induced pluripotent stem cells (iPSCs) which share characteristics similar to those of ESCs [10, 11]. Researchers are investigating the potential of small molecules to trigger pluripotency in cells. Studies have revealed that small molecules like forskolin (FSK), 2-methyl- 5-hydroxytryptamine, and D4476 are effective in creating small-molecule-mediated induced pluripotent stem cells (SmiPSCs), which can show embryonic stem cell-like features [12, 13]. Recent advances reveal that multiple molecular and epigenetic mechanisms govern the reprogramming of spermatogonial stem cells (SSCs) into pluripotent cells. For instance, DNA hypomethylation, particularly when combined with p53 depletion, can induce pluripotency through the Dmrt1-Sox2 cascade, which up-regulates Oct4, thereby facilitating pluripotency [14]. In parallel, chromatin accessibility analyses comparing p53 wild-type and knockout SSCs have highlighted that p53 deficiency predisposes SSCs to reprogramming, with SMAD3 playing a pivotal role [15]. Furthermore, the development of an efficient transformation system incorporating extrinsic factors such as EGF, LIF, and feeder cells—supplemented by small molecule inhibitors (e.g., 2i)—has significantly enhanced pluripotency conversion [16]. Moreover, the selective modulation of epigenetic regulators, particularly through second-generation class I HDAC inhibitors, further increases the reprogramming efficiency [17]. ES-like cells can additionally be produced from SSCs without adding transcription factors, exogenous oncogenes, chemicals, or small molecules in a time-related mechanism in vitro [18]. Reports regarding this mechanism have been documented in both human and murine experiments [19]. ES-like cells from SSCs follow a natural pathway that preserves developmental cues and minimizes genomic instability, unlike iPSCs, which require extensive reprogramming. SSC-derived cells also have an autologous origin, reducing mutation risks and immune rejection, making them a safer and more reliable option for regenerative medicine. However, it has been shown that this derivation has a low occurrence rate of approximately (1 in 1.5 $\times$10^7) in murine [16]. Generating ES-like cells from SSCs provides unique advantages compared to induced pluripotent stem cells (iPSCs), particularly in biological and clinical settings. SSCs possess intrinsic pluripotency potential and can be induced into pluripotent stem cells under specific conditions without the extensive genetic modification typically required for iPSCs, minimizing safety concerns related to mutagenesis. This feature makes SSC-derived pluripotent cells more suitable for clinical applications, such as fertility preservation, especially for prepubescent cancer patients. SSCs also retain epigenetic memory, which can enhance their differentiation potential into germline and related cell types. These properties make SSC-derived stem cells a promising tool in developmental biology and regenerative medicine, especially for applications involving male fertility and reduced genetic manipulation.

The mechanism is regulated by both activated and deactivated genes, which control or influence biological signaling pathways. A comprehensive understanding of the differentially expressed genes and the changes in signaling pathways would shed light on the underlying mechanisms of the derivation of ES-like cells from SSCs. This information could potentially lead us to develop more efficient methods with a higher frequency of ES-like cell generation, enhancing their utility in research and clinical applications. In this research, we delved into the complex transduction pathways that regulate a cell's fate and function. We examined a limited set of genes and analyzed the intricate interplay of numerous significant genes using high-throughput data to explore their connections and interactions. Our computational analyses,

coupled with in vitro experiments and a thorough review of existing literature, allowed us to produce insights that can serve for future experiments and further research. We used microarray data to identify DEGs between two cell groups and constructed a PPI network for functional enrichment analysis. Given microarray limitations in reproducibility and sensitivity, we validated key findings through Fluidigm qPCR, immunofluorescence, and a literature review. In silico and in vitro analyses highlighted cell cycle regulation (NEK kinases, APC/C phosphorylation, G2/M transition) and signaling pathways (PI3 K/Akt, MAPK, SMAD binding, GDNF/RET). Predicted miRNAs and lncRNAs may regulate these processes in ES-like cell derivation from SSCs. We highlight the predicted non-coding RNAs, including miRNAs and lncRNAs, gathered by in silico analysis. These non-coding RNAs can potentially regulate the mechanism underlying the derivation of ES-like cells from SSCs. Understanding these regulatory mechanisms could provide valuable insights into the intricate molecular processes involved in this cellular transition alongside enrichment analysis. By investigating the involvement of non-coding RNAs, our study enhances the comprehensive understanding of the regulatory networks governing stem cell biology. It opens up new paths for further experiments in this field.

Materials and methods

Isolation of spermatogonial stem cells

In this study, animal experiments were conducted with the approval of the Institutional Animal Care and Ethics Committee at Amol University of Special Modern Technologies. All procedures were approved by Heidelberg University's Institutional Animal Care and Use Committee. We used GFP transgenic mice with an Oct4-promoter reporter of the C57BL/6 strain for obtaining testicular cells. The mice were euthanized with CO_2 gas and introduced into the chamber at a regulated flow rate of about 30–70% of the chamber volume per minute to ensure a humane and gradual induction of unconsciousness. Mice were observed to verify unconsciousness before respiration ceased. This method was selected for its effectiveness and broad acceptance as a humane approach to rodent euthanasia. No supplementary anesthetics were administered. The cells were isolated through a single-step enzymatic digestion procedure. The testicular tissue was digested using an enzymatic solution with Collagenase IV, Dispase, DNase, and HBSS buffer at 37 °C for 8 min. The enzymatic digestion was stopped by adding 10% ES cell-qualified FBS and gently pipetting to achieve a single-cell suspension. After centrifugation, the samples were washed with DMEM/F12 medium, filtered through a 70 µm cell strainer, and centrifuged again at 1500 rpm (277 RCF) for 10 min [20].

Culture of spermatogonial stem cells

The suspended testicular cells were plated onto culture dishes coated with 0.2% gelatin after enzymatic digestion. These cells were then cultured in a mouse germline stem cell (mGSC) medium. This medium consisted of StemPro- 34 base medium, supplemented with N2, D+ glucose, bovine serum albumin, L-glutamine, β-mercaptoethanol, penicillin/streptomycin, MEM vitamins, non-essential amino acids (NEAA), estradiol, progesterone, EGF, FGF, GDNF, 100 U/ml LIF, 1% embryonic stem cell-qualified fetal bovine serum (1% ES cell-qualified-FBS), ascorbic acid, pyruvic acid, and DL-lactic acid. The cultures were incubated at 37 °C in a 5% CO2 atmosphere to promote cell growth and viability [20].

Generation and culture of ES-like cells derived from spermatogonial stem cells

In our earlier work, transgenic mice with a GFP reporter linked to the OCT4 promoter from the C57BL/6 strain were cultured in a mouse spermatogonial stem cell medium. In the days of 41–125 after starting the culture, we successfully generated ES-like cells with high expression levels of OCT4-GFP. These cells were then isolated and cultured in a mESCs medium containing KO-DMEM (or high-glucose DMEM), 15% fetal bovine serum (15% FBS), MEM non-essential amino acids (NEAA), L-glutamine, Penicillin–Streptomycin (Pen-Strep), β-mercaptoethanol, and 1000 U/ml of leukemia inhibitory factor (LIF), where they were grown on mouse embryonic fibroblast feeder layers and passaged every few days for continued growth [20].

Teratoma assay

To assess the in vivo differentiation potential of ES-like cells, chimera formation was performed. Blastocysts were collected from superovulated NMRI female mice 3.5 days post-coitus using basic M2 medium. Each blastocyst received approximately 10–15 single ES-like cells. Around 10 injected embryos were then surgically implanted into the uterine horns of pseudo-pregnant NMRI female recipients. Chimeric mice were typically identified based on their coat color [20].

Generation of chimeric mice

Following trypsinization, the ES-like cells were dissociated and replated on plates coated with 0.1% gelatin in an mESC culture medium. The cells were incubated for 1 h at 37 °C in a 5% CO2 environment, after which the supernatant was collected. The cells were then centrifuged and resuspended in a mixture of 130 µL PBS and 70 µL Matrigel, kept on ice. Approximately 2–3 million cells

were subcutaneously injected into 7-week-old SCID-beige mice. Tumor growth was monitored three times per week to assess teratoma formation [20].

Immunocytochemical staining

Testicular cells were subjected to a detailed fixation process using a 4% paraformaldehyde solution, followed by permeabilization with a 0.1% Triton X- 100 solution in PBS. The 1% BSA solution in PBS prevents non-specific binding as a blocking step. Primary antibodies against OCT4 (Santa Cruz Biotechnology, USA), SOX2 (Abcam, UK), PLZF (Merck, Germany), VIM (Sigma-Aldrich, USA), VASA (Abcam, UK), SOX9 (Linaris, Germany), and DAZL (Bio-Rad, USA) were applied for both immunohistochemistry and immunocytochemistry assays. After incubation with the primary antibodies, secondary antibody (goat anti-mouse IgG H&L(Abcam)) was utilized. The 4′,6-diamidino- 2-phenylindole (DAPI) (0.2 g/ml) for 3 min at room temperature and fixed with polyvinyl alcohol (Mowiol) for nuclear counterstaining of the cells. Positively labeled cells were imaged using a confocal Zeiss LSM 700 microscope (Carl Zeiss, Germany), with images captured by a Zeiss LSM-TPMT camera [20].

Fluidigm qPCR gene expression analysis

Quantification of SSCs, ES-like cells, and Mouse Embryonic Fibroblasts (MEFs, used as controls) gene expression was conducted using Fluidigm dynamic array chips. As in our previous experiments [20]. The procedures for gene normalization, cell selection, mRNA reverse transcription, pre-amplification, and quantification using TaqMan qPCR on the BioMark system were followed. Each sample was analyzed in two technical replicates and three biological replicates. GAPDH was used for normalization. Data analysis was performed using GenEx software (v.7.0), Excel, and SPSS.

Microarray data analysis and data normalization

We used the NCBI Gene Expression Omnibus (https://www.ncbi.nlm.nih.gov/geo/) for obtaining the ES-like cell samples and ESC samples from the GSE43850 dataset, alongside SSC expression data from the GSE27043 dataset for microarray analysis. The analysis was performed using the Transcriptome Analysis Console (TAC) software, version 4.0, on the GPL6244 platform (MoGene- 1_0-st). Data was normalized using the Robust Multi-array Average (RMA) method, and differential gene expression was assessed through the empirical Bayes (eBayes) ANOVA method. The crucial differentially expressed genes (DEGs) in this analysis were those with a *P*-value (*P*-value) <0.05 and a fold change beyond -2 or 2 [21].

Protein–protein interaction (PPI) networks and protein clustering

The STRING database (version 12.0) (https://string-db.org/) was employed for protein–protein interactions (PPI) prediction based on Experiments, Text Mining, Neighborhood, Gene Fusion, Co-expression, Databases, and Co-occurrence among the differentially expressed genes (DEGs) identified in this study. The analysis used *Mus musculus* as the reference species, with a medium confidence score threshold of 0.4. The resulting network, which integrated data, was analyzed using Cytoscape (version 3.6.0), Centiscape (version 2.2) plugin, and Gephi application (version 0.10.1) as in our previous study [21].

Enrichment analysis

Enrichment analysis was carried out using the STRING app's enrichment analysis tool to better understand the functional clusters (modules) associated with each protein and the differentially expressed genes (DEGs) within the network. The analysis drew on data from multiple sources, including KEGG, WikiPathways, Reactome, and Gene Ontology (GO) terms, to identify significant enrichment results [21].

mRNA-lncRNA-miRNA network

To assess the influence of miRNA networks on the selected genes, data were gathered from miRDB (https://mirdb.org/mirdb), TargetScan (https://www.targetscan.org/), and RNAInter (http://www.rnainter.org/). The top 10 miRNAs common across these three datasets were identified based on their scores, and a network was constructed using Cytoscape software. For lncRNA data, RNAInter (http://www.rnainter.org/) was also utilized, and the top 10 lncRNAs, ranked by score, were incorporated into the network [21].

Statistical analysis

The experiments were repeated at least three times to ensure reproducibility. Statistical analysis was performed using Statistical Package for the Social Sciences (SPSS) version 27.0. The normality of the gene expression data was assessed using the Shapiro–Wilk normality test. Since the data did not follow a normal distribution, non-parametric tests were employed. Specifically, the Kruskal–Wallis H test was used to compare multiple independent groups. Post-hoc pairwise comparisons were conducted, with the Bonferroni correction applied to adjust for multiple comparisons. For normally distributed data, one-way ANOVA was used instead of the Kruskal–Wallis test, followed by the Bonferroni correction for pairwise comparisons. Statistical

significance was determined when the p-value was < 0.05.

Results

Isolation of SSCs and derivation of ES-like cells from SSCs

Using the Oct4-GFP transgenic mouse model, we isolated spermatogonial stem cells (SSCs) from adult mouse testes. The Oct4-GFP signal was initially observed in the seminiferous tubules (Fig. 1A), which were enzymatically dissociated using collagenase/dispase to obtain a single-cell suspension. The cells were then cultured in mGSC medium, where SSCs appeared between days 2 and 14 as small, round, and compact cells forming tightly packed colonies. Initially, some SSCs exhibited low Oct4-GFP expression, which gradually diminished during long-term culture. However, upon induction of pluripotency, the Oct4-GFP signal was reactivated. During extended culture, a few colonies resembling mouse embryonic stem cells (mESCs) emerged, displaying ES-like morphology. These colonies exhibited a spindle-to-round shape with smooth edges and strongly expressed Oct4-GFP, similar to epiblast-derived cells (Fig. 1B) [20].

Chimera formation following injection of ES-like cells into blastocysts

To determine whether ES-like cells resemble ESCs in contributing to embryonic development in vivo, we examined chimera formation by injecting GSCs into mouse blastocysts. Using a micromanipulator, 10–15 single ES-like cells were selected and injected into 3.5-day-old mouse blastocysts. The injected embryos were then transferred into the uterus of pseudo-pregnant recipient females and allowed to gestate for 18 days. Chimerism in the resulting pups was assessed based on coat color, with some displaying patches of both the host embryo's coat color and the respective ES-like cell clone (Supplementary Figure S1).

Teratoma formation and tri-lineage differentiation confirms pluripotency of ES-like Cells

The formation of teratomas is a key functional assay used to validate pluripotency in stem cell research. In our study, the pluripotency of ES-like cells was assessed by subcutaneously injecting approximately 2 million ES-like cells into five NOD SCID mice. Four weeks post-transplantation, teratomas were observed in all five recipient mice, while no tumors developed in the control group, which only received Matrigel. The injected ES-like cells differentiate into all three germ layers and form complex teratomas in SCID mice. Hematoxylin and eosin (H&E) staining of the teratomas revealed well-differentiated structures originating from the ectoderm, mesoderm, and endoderm. The teratomas formed from the ES-like cells represented all three germ layers (Supplementary Figure S2). The successful formation of teratomas and tri-lineage differentiation confirms the pluripotency of the ES-like cells in this study. The consistent teratoma formation in all five NOD SCID mice, alongside the absence of tumors in the control group, supports the stem-like properties of the injected cells. The differentiation into all three germ layers (ectoderm, mesoderm, and endoderm) further validates their pluripotent potential. These findings, coupled with the ability of the ES-like cells to generate chimeric mice, provide robust evidence for their pluripotency and potential for regenerative applications.

Immunostaining reveals presence of stemness markers in ES-like cells compared to SSCs

The immunostaining method gives us a qualitative view of the expression of selected genes. Both immunocytochemistry (ICC) and immunohistochemistry (IHC) methods were employed in this study. We used immunocytochemistry (ICC) to compare the gene expression rate of OCT4, SOX2, PLZF, Vimentin, and DAZL between ES-like cells and SSCs (Fig. 2). Based on the

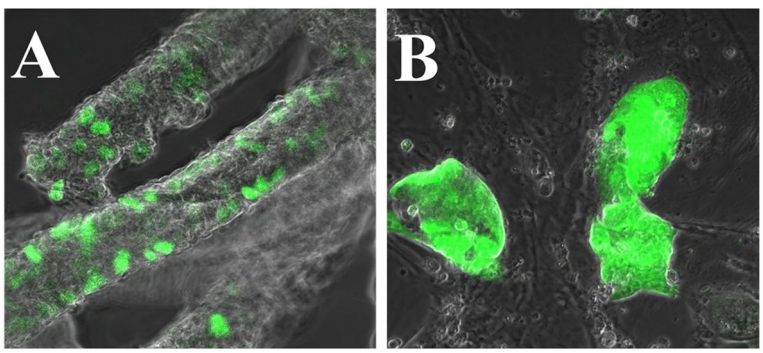

Fig. 1 Oct4-GFP expression in seminiferous tubules and derived ES-like cells. **A** Seminiferous tubules of an Oct4-GFP reporter adult transgenic mouse show Oct4-GFP expression. **B** Derivation and proliferation of ES-like cells exhibiting Oct4-GFP expression in a mouse ESC culture medium. (Scale bar = 50μm)

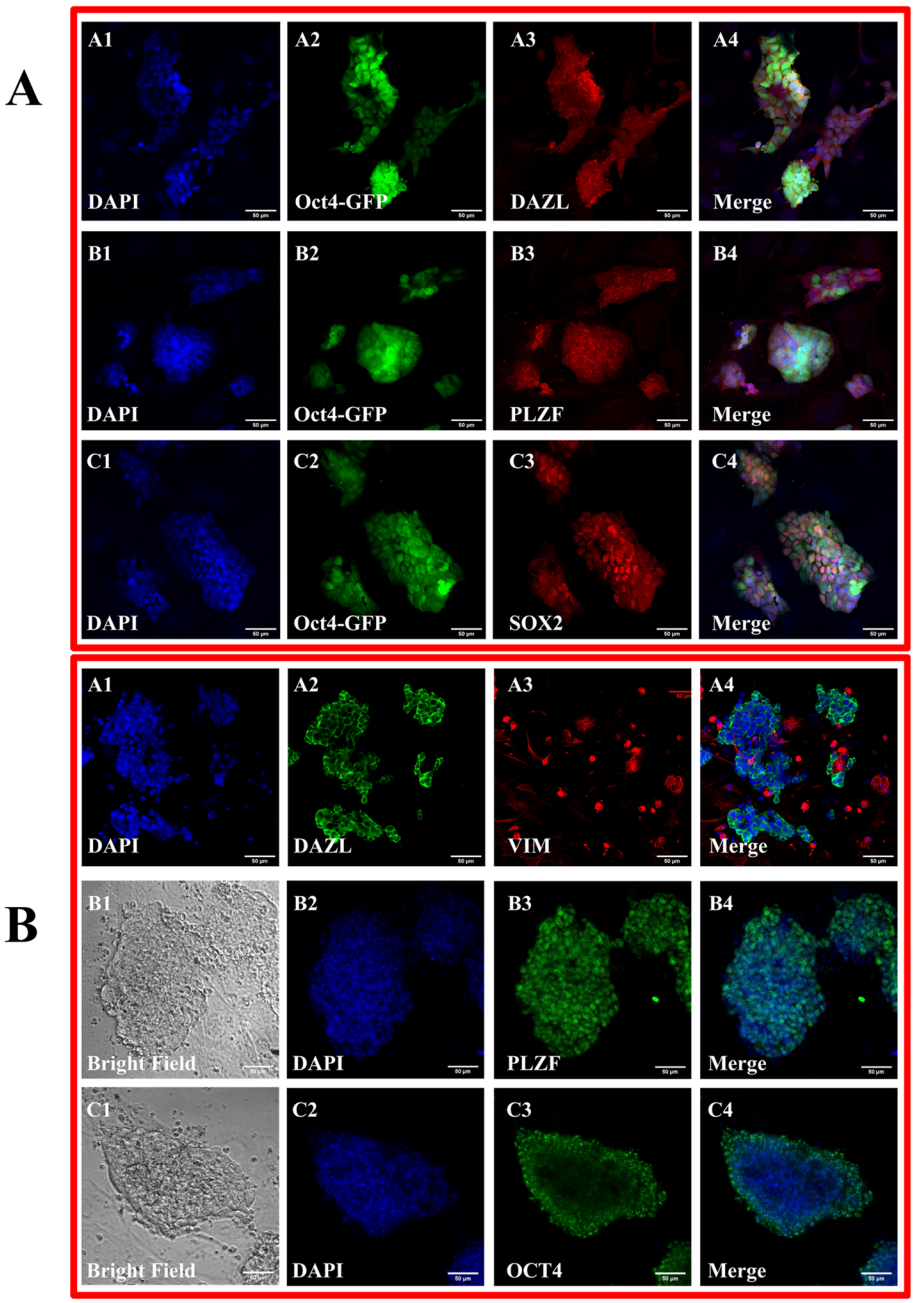

Fig. 2 Immunocytochemical analysis of ES-like cells and spermatogonial stem cells (SSCs). This figure illustrates the expression patterns of key pluripotency and germline markers in ES-like cells and SSCs, as determined by immunocytochemistry (ICC). DAPI (blue) marks nuclei and Oct4-GFP (green) identifies Oct4-expressing cells. **A** Immunocytochemical (ICC) analysis of the ES-like cells for the selected proteins, including DZL (A1-A4), PLZF (B1-B4), and SOX2(C1-C4). The observing ES-like cells are negative for DAZL and PLZF but positive for SOX2. **B** Immunocytochemical (ICC) analysis of the SSC population. In the first row (A1-A4), blue represents DAPI staining, green indicates the DAZL protein, and red shows the VIM protein. It is concluded from (A1-A4) that DAZL-positive SSCs do not express VIM. Images display PLZF (B1-B4) and OCT4 (C1-C4), which are both positive in observed SSCs. Additionally, brightfield images of these cell populations are included as the first image of each group (Scale bar = 50 µm)

immunocytochemistry (ICC) test, SSC-derived ES-like cells were positive for OCT4 and SOX2, showing their stemness properties. However, the absence of PLZF and DAZL expression in ES-like cells suggests that these cells may not fully resemble SSCs, supporting their unique identity as ES-like cells. Additionally, the DAZL-positive

SSCs exhibited negative staining for VIM, suggesting a potential relationship that warrants further investigation. These findings align with our microarray analysis, which revealed distinct gene expression profiles for these proteins between the two cellular groups.

Furthermore, in this study, we utilized Immunohistochemistry (IHC) to assess the expression of selected genes in a section of normal murine seminiferous tubules (Fig. 3). By this approach, we can investigate gene expression in normal tissue alongside single cells, whose gene expression rate was studied using the immunocytochemistry (ICC) method, within an in vitro setting. IHC analysis of normal murine seminiferous tubules provided additional context by mapping these markers to their endogenous expression patterns. PLZF-positive cells lacked VASA expression, confirming their identity as undifferentiated spermatogonial, while SOX9-positive cells were negative for DAZL, reinforcing the distinct lineage specification. These results not only validate the differential expression of key genes but also highlight the functional divergence between ES-like cells and SSCs.

In Silico transcriptome analysis reveals presence of pluripotency markers in ES-like cells compared to SSCs

We employed Transcriptome Analysis Console (version 4.0) (TAC) to pinpoint differentially expressed genes between the ES-like cells group and the SSCs group. We used the RMA method for normalization, and gene expression criteria were applied with a significance threshold set with a *P*-value <0.05 and a fold change cut-off of <-2 or >2. This analysis revealed 3956 differentially expressed genes (DEGs) between ES-like cells and SSCs based on this criterion (Fig. 4A). Initially, 1615 genes were singled out from 3956 DEGs based on criteria such as lower *p*-value, higher fold change ($-3>$ fold change >3). Within these selected genes, 1031 were observed to be upregulated, while 586 were downregulated in ES-like cells. Notably, key DEGs included *Tdgf1*, *Apela*, *Zic2*, *Nanog*, *Cldn6*, *Dnmt3 l*, *Otx2*, *Stmn2*, *Tet1, Enpp3, Luzp4, Asz1, Pramel3, Taf7 l, Tex11, Xlr5a, Uba1y, Nlrp4c, Mageb4, Xlr5c, and Nxf2* (Fig. 4B). The upregulation of pluripotency-related genes such as Nanog suggests that ES-like cells may retain or exhibit stemness characteristics more prominently than SSCs. Conversely, the downregulated genes likely indicate the suppression of lineage-specific or differentiation-related pathways in ES-like cells.

To validate our findings, we conducted an additional comparative analysis between ESCs and SSCs using the same normalization and selection criteria. This microarray analysis identified 4,433 DEGs, of which 1,773 were selected based on stringent *p*-value and fold-change thresholds ($-3>$ fold change >3). Interestingly, all of the highly differently genes between ES-like cells and SSCs which stated above (*Tdgf1, Apela, Zic2, Nanog, Cldn6, Dnmt3 l, Otx2, Stmn2, Tet1, Enpp3, Luzp4, Asz1, Pramel3, Taf7 l, Tex11, Xlr5a, Uba1y, Nlrp4c, Mageb4, Xlr5c, Nxf2*) were also among the highly differentially

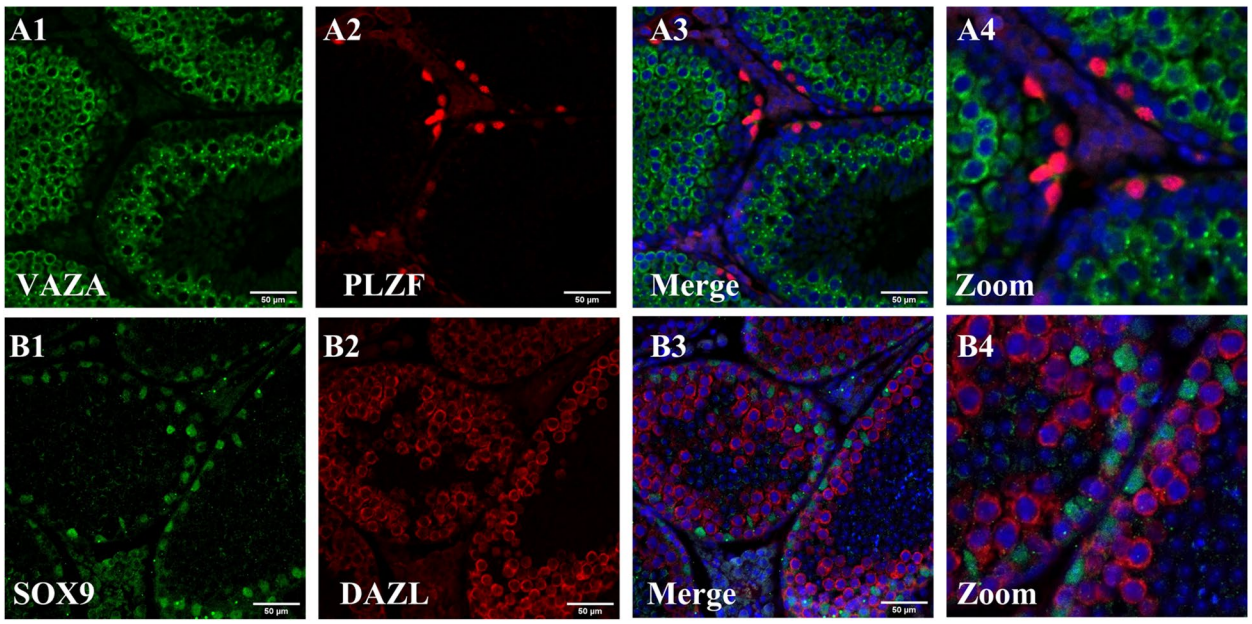

Fig. 3 Immunohistochemistry (IHC) analysis of testis cross-sections revealed specific expression patterns among various cell types. (A1-A4) PLZF-positive cells (red) exhibited no expression for the germ cell marker VASA (green). (B1-B4) SOX9-positive cells (green) were negative for the germ cell marker DAZL (red) (Scale bar = 50 µm)

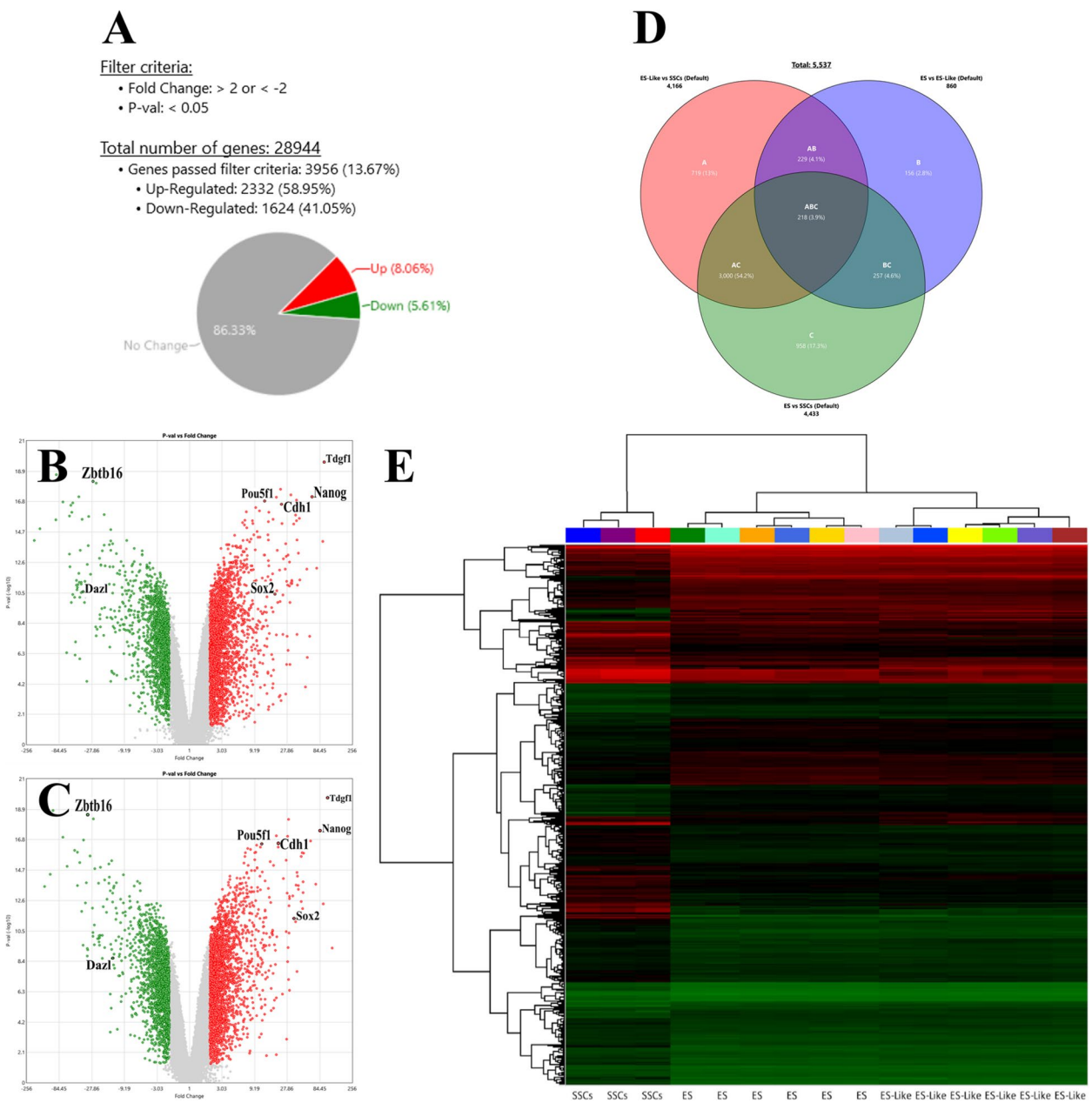

Fig. 4 Transcriptomic comparison of ES-like cells, embryonic stem cells (ESCs), and spermatogonial stem cells (SSCs). This figure summarizes differential gene expression analysis using publicly available microarray datasets: SSCs from GSE27043, and ESCs and ES-like cells from GSE43850. The analysis reveals transcriptional similarities between ES-like cells and ESCs, and key differences compared to SSCs. **A** Overview of the microarray analysis results comparing global expression profiles among ES-like cells and SSCs. **B** Volcano plot showing fold change and *p*-values for differentially expressed genes (DEGs) between ES-like cells and SSCs, with a threshold of *p*-value < 0.05. **C** Volcano plot illustrating DEGs between ESCs and SSCs, highlighting genes with significant transcriptional shifts (*p*-value < 0.05). **D** Venn diagram depicting the number of DEGs and their overlapping intersections among the three cell types. **E** Heatmap of all samples (3 SSCs from GSE27043; 6 ESCs and 6 ES-like cells from GSE43850), showing clustering patterns. ES-like cells exhibit gene expression profiles closely resembling those of ESCs

expressed genes in the ESCs vs. SSCs comparison (Figs. 4C).

For visualization, we generated a Venn diagram and, heatmap plot highlighting common DEGs across these analyses (Fig. 4D, E). Our findings revealed a strong similarity in gene expression patterns between ESCs and ES-like cells. The observed similarity, although not a perfect match, reassured us that the ES-like cells possess a

pluripotent identity, consistent with our goal to compare a pluripotent cell type (ES-like cells) with SSCs. While gene expression similarity alone does not guarantee statistical precision in DEG identification, it provides essential biological context. By showing the pluripotent state of the ES-like cells, we ensured that the DEGs identified reflect true differences between pluripotent cells and SSCs rather than artifacts from mischaracterized cells. The differential expression of key regulatory genes such as *Tdgf1*, *Nanog*, and *Tet1* underscores the active modulation of pathways critical for maintaining stem cell characteristics and directing cell fate decisions. This high concordance suggests that ES-like cells retain essential pluripotent properties, reinforcing the reliability of our identified DEGs and providing a solid foundation for further investigation.

In Vitro validation confirms differential expression of key pluripotency genes in ES-like cells

We used quantitative and qualitative in vitro tests to validate our microarray gene expression results. This approach allows us to gain insights into the robustness of our identified DEGs and, consequently, the robustness of our enriched pathways. Fluidigm qPCR was utilized as a quantitative test to measure differences in mRNA expression rates among ES-like cells compared to SSCs. Based on our Fluidigm gene expression data, we observed significant differences in the expression patterns of *Dppa5, Cdh1, Pou5f1 (OCT4), Zbtb16 (PLZF), Piwil2, CD9, Nanog, Dazl, Thy1 and Tdgf1* between ES-like cells and SSCs (Fig. 5). These differences in gene expression validate, to some extent, our computational analysis. However, no significant difference was observed in the expression patterns of *Vim* between these two cellular groups.

Network analysis reveals 70 hubs and four distinct functional protein clusters from DEGs

We gave the 1615 filtered DEGs between test groups from the previous stage to the STRING database for building a protein–protein interaction (PPI) network. In the next step, we used Cytoscape (v.3.6.0) to analyze the constructed network based on network parameters. Centrality is a key concept in network analysis that helps identify the vital nodes within a network. Node importance can be measured in several ways. Different centrality measures, such as degree centrality, closeness centrality, betweenness centrality, and eigenvector

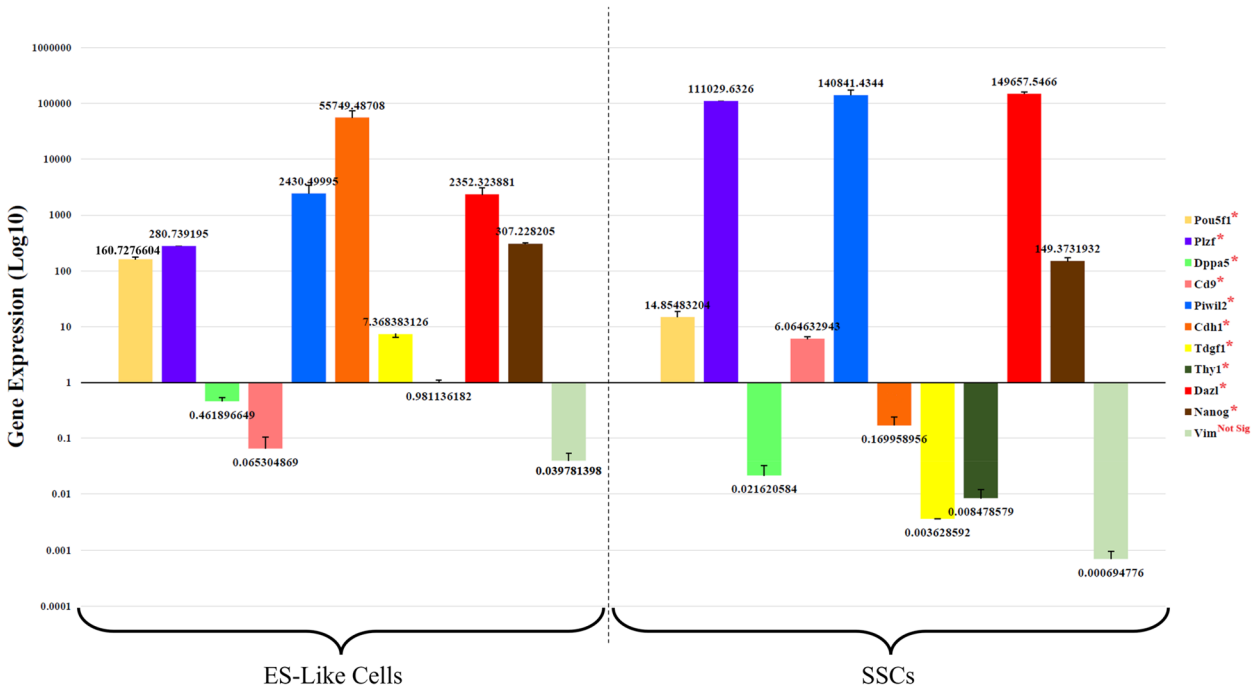

Fig. 5 Gene expression profiling during the transition of SSCs into ES-like cells using Fluidigm qPCR analysis. This figure shows the relative fold change in mRNA expression (Y-axis) for a panel of pluripotency and germline-associated genes during the reprogramming of spermatogonial stem cells (SSCs) into ES-like cells. Expression levels were normalized to mouse embryonic fibroblasts (MEFs), used as the reference population. Asterisks ("*") indicate statistically significant differences in gene expression compared to the MEF group ($p < 0.05$). Significant upregulation was observed in *Dppa5, Cdh1, Pou5f1* (OCT4), *Zbtb16* (PLZF), *Piwil2, CD9, Nanog, Dazl, Thy1, and Tdgf1*, reflecting activation of pluripotency and germline programs. *Vim* expression, however, did not show a significant change, suggesting it is not involved in this transition

centrality, each highlight distinct aspects of a node's role within a network. So, the most important DEGs were filtered through the network among 1615 nodes based on different centrality parameters. We applied node filtering to retain the most important and relevant nodes while ensuring that the number of nodes does not become very low, as this could negatively impact the comprehensiveness of our analysis and limit the scope of our pathway analysis research (Supplementary Figure S3). This approach allows us to analyze comprehensively while focusing on key elements. This method will enable us to identify pivotal genes essential for network connectivity.

As a result, 70 hub genes were identified within the PPI network with significant Adj. *p*-values (Supplementary Figure S4 and S5). These proteins are predicted to play a key role in stemness-related pathways in ES-like cells compared to SSCs. However, in a biological context, they do not function in isolation but rather operate within modules to drive specific pathways. Modularity analysis highlights that these hub genes act within coordinated networks, revealing the intricate interplay governing gene regulation in stem cells. This systematic approach not only refines pathway analysis by identifying pivotal nodes but also deepens our understanding of the coordinated molecular interactions underlying the studied biological condition. These hub genes were then subjected to modularity analysis and protein cluster (Modules) formation using Gephi (version 2.2). Through Gephi's built-in modularity algorithm, four distinct protein clusters (Modules) emerged from a network of 70 hub proteins. Cluster (Module) 1 consists of 21 nodes; Cluster (Module) 2 has 16 nodes; Cluster (Module) 3 consists of 12 nodes, and the last cluster (Module) has 21 nodes (Fig. 6). Each cluster (Module) signifies proteins that work together to fulfill specific functions in the differentiation path of SSCs to the ES-like. This enables us not only to examine enriched pathways involving all the present DEGs within the network but also to delve deeper into the functions of individual proteins and their closely collaborating partner genes within this pathway.

Enrichment analysis of four protein clusters uncovers key pathways in ES-like cell function

We performed independent enrichment analyses for each protein cluster (module) to obtain detailed and precise results. Genes within each cluster were imported into the STRING database (*Mus musculus*) to construct protein–protein interaction (PPI) networks and perform functional enrichment analyses using Gene Ontology (GO), KEGG, Reactome, and Wikipathways databases (Table 1). We prioritized the top 10 pathways based on strength and False Discovery Rate (FDR) ($p < 0.05$) and further examined pathways with lower Adj. *P*-value to capture additional biological insights. This approach enabled us to focus on the most significant pathways while also considering less prominent but potentially important findings.

The first identified cluster is enriched in key transcription factors (TFs) and microRNAs (miRNAs) governing stem cell regulation, particularly in iPS cell generation and pluripotency maintenance. Functional enrichment analysis highlights its association with the GDNF/RET signaling axis, DNA methylation, Wnt signaling, and retinoic acid response, all of which are fundamental to stem cell fate determination. Notably, the presence of core pluripotency factors (SOX2, OCT4, and NANOG) underscores its role in maintaining stemness and self-renewal. Additionally, epigenetic regulators such as Dnmt3b and Dnmt3 l reinforce the significance of DNA methylation in stem cell identity. The enrichment of signaling pathways regulating pluripotency, along with factors involved in stem cell division and population maintenance, suggests that this cluster serves as a functional module orchestrating the balance between self-renewal and differentiation.

The second cluster is highly enriched in cell cycle regulation, DNA damage response, and histone modifications, emphasizing its role in cell proliferation and genomic stability. Key regulators such as CDK1, CCNE1, and PLK1 highlight its involvement in G2/M transition and mitotic progression, while TP53-regulated transcriptional programs, APC/C phosphorylation, and Emi1 phosphorylation suggest stringent checkpoint control mechanisms to maintain genomic integrity. Additionally, the presence of histone demethylases (HDMs) and histone variants (H2 AX, H2 AZ1, H3 C7, H4 C11) underscores the cluster's role in epigenetic regulation and chromatin remodeling. The inclusion of BMI1, a Polycomb repressive complex component, further supports its function in transcriptional repression during the cell cycle.

This cluster is strongly associated with ECM remodeling, cell adhesion, and collagen metabolism, suggesting a key role in tissue integrity and cellular motility. Pathway analysis highlights collagen biosynthesis, degradation, fibril organization, and matrix metalloproteinase (MMP)-mediated ECM turnover, driven by components such as MMP9 and MMP3. The inclusion of COL1 A2 and COL3 A1 suggests an active collagen network, while LU and THBS1 indicate roles in collagen fibril assembly and ECM-cell adhesion. Given the interplay between collagen synthesis, degradation, and integrin-mediated interactions, this cluster likely modulates cellular plasticity and niche remodeling, with potential implications in stem cell niches.

The fourth cluster is highly enriched in FGFR-mediated signaling, particularly FGFR1 and FGFR2 pathways, which

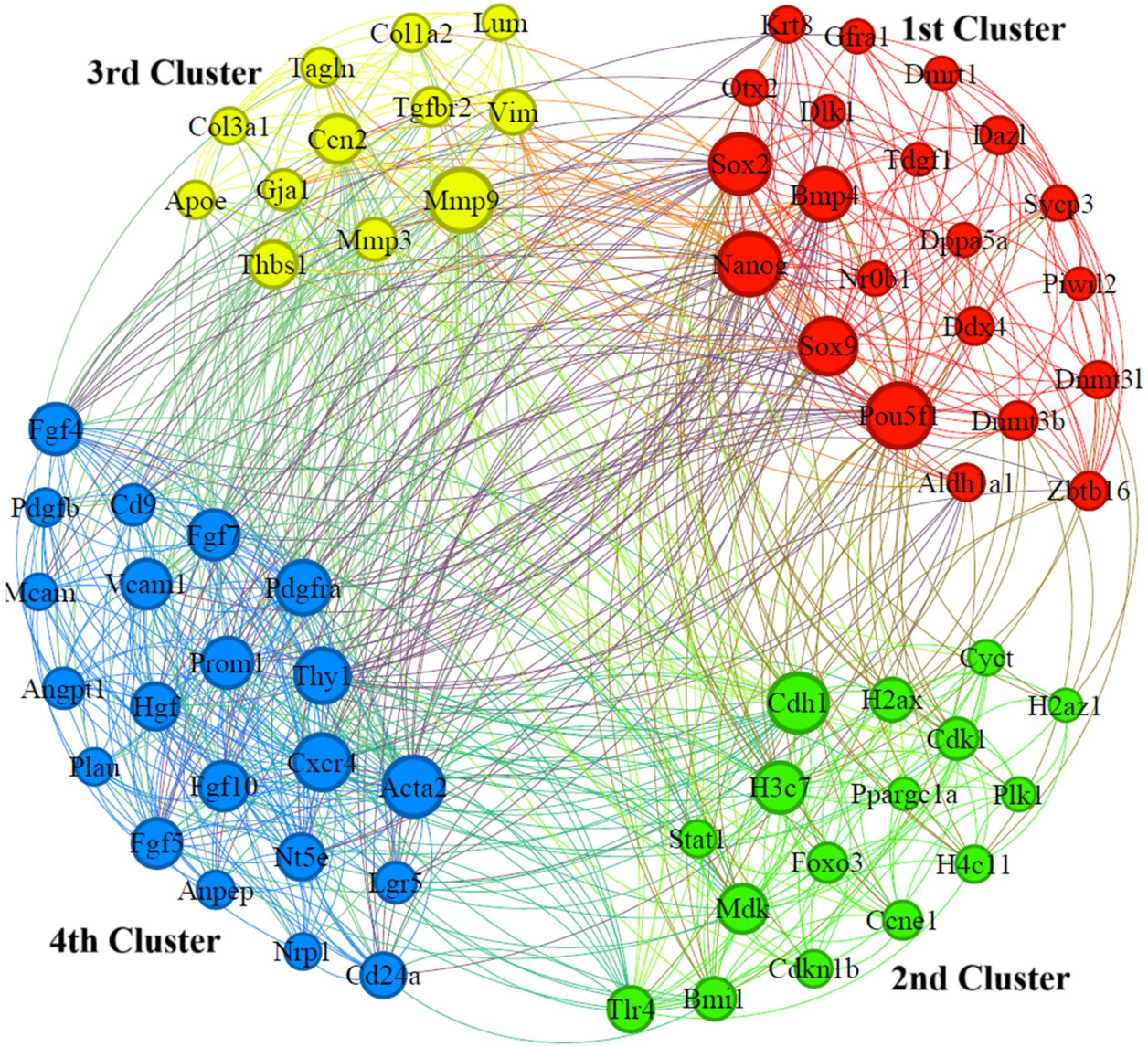

Fig. 6 Protein–protein interaction (PPI) network analysis reveals four distinct functional clusters. The PPI network was constructed and analyzed using Gephi, where clustering algorithms and filters were applied to identify hub proteins and their interacting neighbors. The network is organized into four distinct clusters, each represented by a different color, indicating functional groupings. Node size corresponds to connectivity (degree), where larger nodes represent hub proteins with higher interaction counts, highlighting their potential regulatory importance within each cluster. This visualization reflects how hub proteins may coordinate key biological processes in their respective pathways

are critical for cell proliferation, differentiation, and tissue regeneration. The presence of multiple FGFs (FGF4, FGF5, FGF7, FGF10) and receptor modulators (FGFRL1, NRP1) suggests active regulation of PI3 K, SHC, and FRS-mediated pathways, which govern cell survival and migration. Markers such as LGR5, PROM1 (CD133), and CD24 A indicate potential involvement in stem cell maintenance and epithelial-mesenchymal interactions. Additionally, HGF (hepatocyte growth factor) and CXCR4 support roles in stem cell niche dynamics and migration, while ANPEP (CD13) and NT5E (CD73) link this network to stem cell plasticity, adenosine metabolism, and immunomodulation to stem cell maintenance, extracellular adenosine metabolism, and immunomodulation, which may influence stem cell plasticity and microenvironmental crosstalk.

mRNA-lncRNA-miRNA network analysis identifies key regulatory RNAs to enhance ES-like cell generation efficiency

We selected a list of genes exhibiting a validated differential expression pattern through Fluidigm qPCR analysis and immunostaining tests, including *Dazl*, *Pou5f1*,

Table 1 Top 10 enriched pathways within each predicted protein functional cluster

1st Cluster		
Enriched Pathways	**false discovery rate**	**strength**
miRNAs and TFs in iPS Cell Generation	0.0021	2.47
GDNF/RET signaling axis	0.0095	1.98
Negative regulation of miRNA transcription	0.0189	1.94
DNA methylation	7.62E-05	1.89
Stem cell division	0.0293	1.81
Stem cell population maintenance	8.70E-05	1.54
Response to retinoic acid	0.00088	1.54
Mechanisms associated with pluripotency	6.87E-10	1.51
Wnt signaling pathway and pluripotency	0.0058	1.51
Signaling pathways regulating pluripotency of stem cells	0.0031	1.48
2nd Cluster		
Enriched Pathways	**false discovery rate**	**strength**
Activation of NIMA Kinases NEK9, NEK6, NEK7	0.00088	2.74
Phosphorylation of Emi1	0.0011	2.66
PTK6 Regulates Cell Cycle	0.0011	2.66
TP53 Regulates Transcription of Genes Involved in G1 Cell Cycle Arrest	0.0022	2.44
Phosphorylation of the APC/C	0.0072	2.14
Positive regulation of reactive oxygen species biosynthetic process	0.0264	2.06
Cyclin A/B1/B2 associated events during G2/M transition	0.0094	2.06
HDMs demethylate histones	0.0095	2.04
Type II interferon signaling (IFNG)	0.013	1.94
FLT3 Signaling	0.0141	1.93
3rd Cluster		
Enriched Pathways	**false discovery rate**	**strength**
MET activates PTK2 signaling	0.013	2.24
Assembly of collagen fibrils and other multimeric structures	1.17E-05	2.18
Collagen degradation	1.31E-05	2.12
Matrix metalloproteinases	0.0052	2.11
Positive regulation of collagen biosynthetic process	0.0215	2.06
Non-integrin membrane-ECM interactions	0.0258	2.06
Activation of Matrix Metalloproteinases	0.0258	2.02
Collagen fibril organization	0.0024	2
Integrin cell surface interactions	2.90E-05	2
Collagen chain trimerization	0.0258	2
4th Cluster		
Enriched Pathways	**false discovery rate**	**strength**
FGFRL1 modulation of FGFR1 signaling	0.000031	2.38
Phospholipase C-mediated cascade; FGFR2	0.000000853	2.36
FGFR2b ligand binding and activation	0.0023	2.36
FGFR2 ligand binding and activation	0.000000924	2.34
FGFR1 ligand binding and activation	0.0000415	2.32
Phospholipase C-mediated cascade: FGFR1	0.0000473	2.29
FGFR1c ligand binding and activation	0.0032	2.28
PI-3K cascade:FGFR2	0.00000166	2.26
SHC-mediated cascade:FGFR2	0.00000166	2.26
FRS-mediated FGFR2 signaling	0.0000019	2.22

Foxo3, *Piwil2*, *Sox2*, *Zbtb16*, *Nanog*, *Cdh1*, *Dppa5*, and *Cd9* (Fig. 7). The construction of the mRNA-lncRNA-miRNA network serves as a tool to identify miRNAs or lncRNAs that impact specific individual mRNAs or a set of mRNAs. By integrating differentially expressed genes validated through Fluidigm qPCR and immunostaining tests, we constructed a regulatory network that highlights potential post-transcriptional modulators of key pluripotency-related genes. This approach allowed us to identify miRNAs and lncRNAs that may either enhance or inhibit the efficiency of ES-like cell generation, offering potential targets for further experimental validation.

The most relevant miRNAs were predicted and chosen for network construction using data from miRDB, TargetScan, and RNAInter databases. These datasets were then imported and visualized as a network using the Cytoscape app. Our analysis identified several miRNAs (e.g., mmu-miR- 26b- 5p, mmu-miR- 9- 5p, mmu-miR-30b- 5p, mmu-miR- 127 - 3p, and mmu-miR- 452 - 3p) and lncRNAs (e.g., Pantr1, Hotair, Xist, Tsix, and Dalir) that are predicted to regulate genes crucial for pluripotency. These findings suggest that the interplay between miRNAs and lncRNAs plays a critical role in fine-tuning gene expression during ES-like cell generation, either by promoting or repressing specific transcriptional programs.

The identification of these regulatory RNAs provides a foundation for future studies aimed at optimizing reprogramming conditions and improving the efficiency of ES-like cell derivation. By experimentally validating these interactions, we can refine our understanding of the molecular mechanisms governing pluripotency induction and potentially enhance protocols for generating stem-like cells with higher efficiency and stability.

Discussion

This study investigated the gene expression profiles and molecular mechanisms underlying the derivation of pluripotent ES-like stem cells from spermatogonial stem cells (SSCs) using microarray analysis, validated by in vitro assays. Unlike iPSCs, which require extensive reprogramming of differentiated cells—a process that can introduce genomic instability such as mutations or incomplete epigenetic resetting—SSC-derived ES-like cells follow a natural, time-related pathway that better preserves inherent developmental cues. Unlike ESCs, which raise ethical concerns due to their embryonic origin and face sourcing limitations, SSCs are abundant in adult testicular tissue, making them a practical and ethically preferable option. Their robustness, reliability, and autologous potential minimize immunogenicity and enhance safety, positioning them as a superior choice

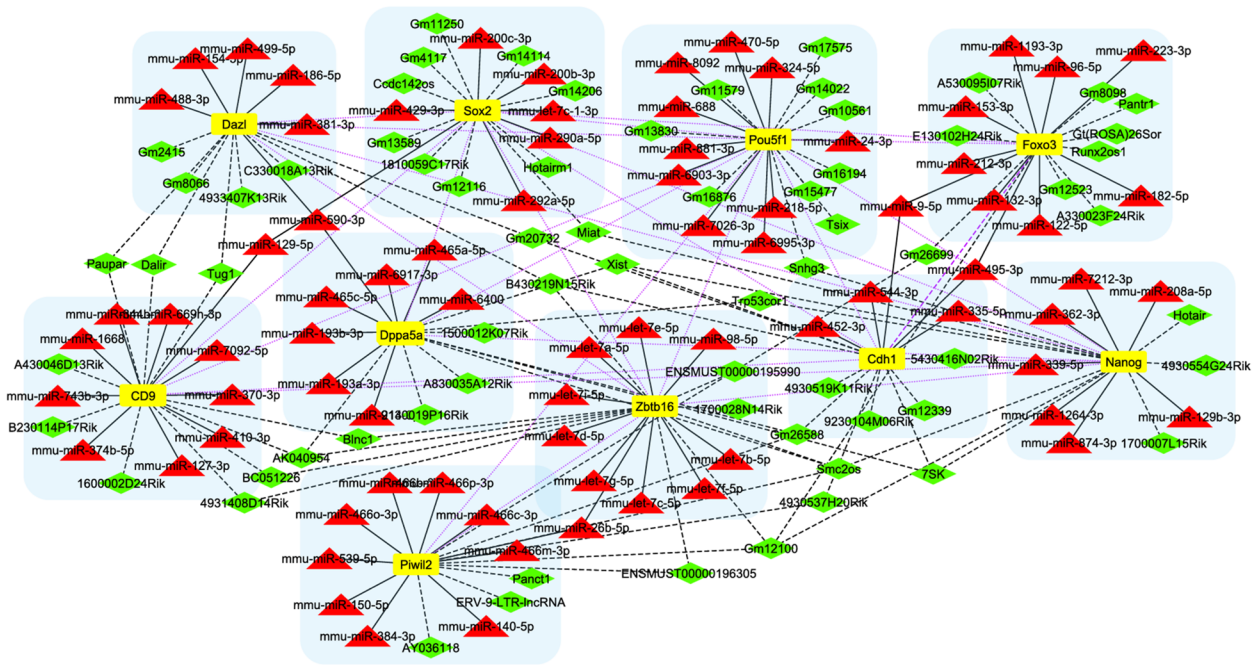

Fig. 7 Visualization of the protein–miRNA–lncRNA network. This figure depicts a bioinformatics-based network showing interactions between proteins, miRNAs, and lncRNAs. Common miRNAs and lncRNAs were identified through integrated analyses, revealing their regulatory relationships with target genes. Yellow rectangles represent target genes, which are connected to related genes by a purple dotted line, based on predictions from previous analyses in this research. Red triangles indicate miRNAs, connected to their target genes by black lines. Green diamonds represent lncRNAs, connected to their target genes by dashed lines

for regenerative medicine applications like tissue repair, organ regeneration, and treating conditions such as infertility or degenerative diseases. We identified 70 critical differentially expressed genes (DEGs) and enriched pathways that distinguish ES-like cells from SSCs, highlighting their shift toward a pluripotent state. Key findings include the significant upregulation of pluripotency markers (*Nanog, Pou5f1, Sox2*) and downregulation of *Dazl*, alongside the identification of four functional protein clusters linked to stemness, cell cycle regulation, ECM remodeling, and FGF signaling.

The upregulation of *Nanog, Pou5f1, and Sox2* in ES-like cells, validated by Fluidigm qPCR and PPI network analysis, underscores their transition to a pluripotent phenotype. Previous studies have highlighted that *Nanog and Dnmt3b* are essential for mESCs [22, 23]. In human induced pluripotent stem cells (hiPSCs), TDFG1 is highly expressed compared to somatic cells [24]. Additionally, *Pou5f1* was identified as a regulator in the process of deriving ES-like cells from murine SSCs [21]. Our findings also suggest that LGR5 affects SOX2, a connection that might be critical for understanding the role of Sox2 in the pluripotency network, as it has previously been shown that LGR family members, especially LGR4, affect SOX2 in mammary development and stem cell functions [25]. Furthermore, *Sox2* and *Dppa5* overexpression have been shown to regulate ES-like cell derivation from murine SSCs [26, 27]. Notably, the close relationship between OTX2, OCT4, and SOX2 in the PPI network supports previous research indicating that OCT4 and SOX2 regulate OTX2 in hiPSCs [28]. *Vim*, a stemness marker in stem cells [29–31] was upregulated in ES-like cells with a significant Adj. *P*-value in microarray analysis. Given these findings, while *Vim* was identified as a significant DEG in the microarray data, its expression was not confirmed by qPCR. Therefore, its role in SSC-derived ES-like cell pluripotency remains uncertain and may be limited. Conversely, *Dazl*'s marked downregulation suggests a suppression of germ-line identity, potentially enhancing pluripotency by alleviating its reported inhibitory effects on *Oct4, Nanog, and Sox2* [32–34]. Further studies are needed to determine whether this alteration in *Dazl* expression has a direct functional impact on the pluripotency of SSC-derived ES-like cells.

Using computational algorithms, we divided the 70 Differentially Expressed Genes (DEGs) into four functional clusters (Modules) for a more accurate pathway enrichment analysis. These predicted enriched pathways and their involved genes may play a crucial role in ES-like derivation and the pluripotency state of SSC-derived cells. The first cluster highlighted the GDNF/RET and Wnt signaling pathways, both of which are crucial for maintaining stemness. Although the role of GDNF/RET in stem cells has not been extensively studied, it is known to enhance spermatogonial stem cell (SSC) survival by mitigating oxidative stress, which may be pivotal for adapting to pluripotency induction [35–37], while Wnt signaling plays a fundamental role in regulating stem cell self-renewal and metabolism [38, 39]. "Activation of NIMA Kinases NEK9, NEK6, NEK7" was among the significantly enriched terms of highlighted clusters. While NIMA kinases regulate mitosis (Fry et al., 2012), their role in pluripotent stem cells remains unexplored. Notably, reducing NEK2 expression in hepatocellular carcinoma suppresses cancer stem cell traits and stemness genes (*Nanog, Sox2, Bmi- 1*) [40]. This suggests a potential link between NIMA kinases and pluripotency in SSC-derived ES-like cells, warranting further investigation into their regulatory influence. Evidence indicates that ESCs express high levels of Emi1, inhibiting APC/C (Anaphase-Promoting Complex/Cyclosome) activity [41]. The PI3 K/Akt pathway critically supports pluripotency, maintaining the undifferentiated state of hESCs and the viability of iPSCs [42]. As our analysis revealed, the"TGF-beta signaling pathway"and"SMAD binding"are among the enriched pathways of the third cluster. In hESCs, SMAD2/3 serves as the primary effector of the TGFβ/Activin/Nodal signal, playing distinct roles in undifferentiated hESCs compared to committed cells [43]. The fourth cluster appears to primarily regulate the FGF/FGFR signaling pathway, while also influencing the MAPK, Ras, and PI3 K-Akt signaling pathways. The FGF/FGFR signaling pathway is mediated by the RAS/MAPK and PI3 K-Akt pathways [44]. It has been concluded that the FGF2-mediated MAPK signaling pathway is crucial for hiPSCs maintenance [44]. Further investigations are needed to explore the specific role of FGFR4 and its signaling pathway in the context of murine ES-like cells.

In addition to mRNAs, non-coding RNAs such as miRNAs and lncRNAs play an important role in gene regulation and stem cell properties. Our constructed mRNA-lncRNA-miRNA network predicted several miRNAs, such as miR- 127 -3p and miR- 410 -3p, that may influence the pluripotency of ES-like cells. It has been demonstrated that miR- 410 -3p is active in ESCs and promotes the cancer stem cell (CSC) phenotype. Additionally, it is known that the target genes of miR- 410 -3p have context-dependent regulation [45]. It has been mentioned that let-7e is upregulated in ESCs and influences the expression rates of β-catenin [46]. The properties of let- 7e observed in ESCs may also apply to SSCs-derived ES-like cells, as predicted in our analysis. miR- 154 -5p, one of the predicted miRNAs, has been shown to regulate the TGFβ1/SMAD pathway [47] that emerges as one of the predicted enriched pathways in our analysis. There are reports in other stem

cell populations, though not in ES-like cells, suggesting that miR- 140 -5p affects the ERK/MAPK signaling pathway in neural stem cells (NSCs) [48], as well as the influence of hsa-miR- 150 -5p on corneal epithelial stem cells (CESCs) [49]. Moreover, lncRNA Snhg3 regulates mESCs self-renewal and pluripotency by regulating *Nanog* and *Pou5f1* [50]. Although the impact of lncRNA on ES-like cells requires further investigation, there is evidence supporting its influence on other cancer cell types. The lncRNA Miat has been found to regulate *Nanog* and *Sox2* in cancer stem cells, contributing to stemness properties [51]. Similarly, lncRNA Hotair plays a role in regulating stemness pathways in breast cancer stem cells (CSCs) [52].

Conclusion and future perspective

With rapid advancements in the use of stem cells in clinics, there is an uprising need for a reliable source of pluripotent stem cells. ES-like cells are promising in this regard, but generating them in sufficient quantity and quality can be challenging. SSCs have been recognized as a possible source of ES-like cells, though their effectiveness in this role remains limited. We aimed to study the underlying biological pathways involved in the derivation of SSCs to ES-like cells. By identifying DEGs using microarray data and highlighting the effects of miRNAs and lncRNAs on these DEGs and pathways, we aimed to gain insights that could pave the way for future experiments addressing these challenges. The microarray data revealed several genes that are upregulated, including *Tdgf1, Nanog, Cdh1, Otx2, and Sox2,* among others, while genes such as *Dazl, Zbtb16, Piwil2, Fgf7, and Gfra1* were found to be downregulated. These genes significantly enrich pathways such as activation of NIMA kinases, phosphorylation of Emi1, GDNF/RET signaling, DNA methylation, PTK2 signaling, collagen fibril organization, and FGFRs activation, among others, as outlined in the main text. Additionally, miRNAs such as miR- 154 -5p, let- 7, miR- 410 -3p, and miR- 127 -3p, along with lncRNAs including Xist, Hotair, Paupar, Tug1, and Snhg3, are predicted to have regulatory effects on these pathways and the SSCs to ES-like derivation path. By studying the molecular mechanisms controlling this derivation process, our goal is to contribute essential knowledge that will support the development of future studies employing more efficient techniques for generating ES-like cells from SSCs and other potential candidates. This advancement aims to further progress in stem cell research and regenerative medicine.

Supplementary Information

The online version contains supplementary material available at https://doi.org/10.1186/s12864-025-11612-y.

Supplementary Material 1.

Acknowledgements
This research was conducted with the generous support of the Faculty of Biotechnology at Amol University of Special Modern Technologies, Islamic Republic of Iran, and the Institute for Anatomy and Cell Biology III – Department of Neuroanatomy at Heidelberg University, Germany, as part of a collaborative effort established under a memorandum of understanding (MoU) agreement. Additional support was provided through a separate MoU between Amol University of Special Modern Technologies and the Faculty of General Medicine at Koya University, Kurdistan Region, Iraq.

Authors' contributions
N.G. conducted and designed the experiment, managed the bioinformatics data design, assembled and analyzed the data, and wrote and edited the final document. H.A. carried out and designed the experiment and was responsible for project administration. A.Q. provided critical feedback and contributed to data analysis. T.S. provided critical feedback and contributed to data analysis. All authors have read and agreed to the published version of the manuscript.

Funding
Amol University of Special Modern Technologies and Heidelberg University funded this work.

Data availability
The datasets analyzed during the current study are available in the NCBI, GEO repository, GSE27043 (https://www.ncbi.nlm.nih.gov/geo/query/acc.cgi?acc=GSE27043) and GSE43850 (https://www.ncbi.nlm.nih.gov/geo/query/acc.cgi?acc=GSE43850).

Declarations

Ethics approval and consent to participate
The Ethics Committee of Amol University of Special Modern Technologies approved the animal study protocol.

Competing interests
The authors declare no competing interests.

Author details
[1]Department of Applied Biotechnology and System Biology, College of Biotechnology, Amol University of Special Modern Technologies, Amol, Iran. [2]Department of Stem Cells and Cancer, College of Biotechnology, Amol University of Special Modern Technologies, P.O. Box 49767, Amol, Iran. [3]Department of Surgery, Faculty of General of Medicine, Koya University, Koya, Kurdistan Region FR KOY45, Iraq. [4]Institute for Anatomy and Cell Biology, Medical Faculty, University of Heidelberg, Im Neuenheimer Feld 307, Heidelberg 69120, Germany.

Received: 19 October 2024 Accepted: 17 April 2025
Published online: 30 April 2025

References

1. Gill JK, et al. Stem cell therapy for cardiac regeneration: past, present, and future. Can J Physiol Pharmacol. 2024;102(3):161–79.
2. Akbaribazm M. Exploring the Regenerative Potential of Stem Cells for Treating Eye Diseases: A Review of the New Findings. OBM Genetics. 2024;08(01):212.
3. Nourian Dehkordi A, et al. Skin tissue engineering: wound healing based on stem-cell-based therapeutic strategies. Stem Cell Res Ther. 2019;10(1):111.
4. Zeng C-W. Advancing Spinal Cord Injury Treatment through Stem Cell Therapy: A Comprehensive Review of Cell Types, Challenges, and Emerging Technologies in Regenerative Medicine. Int J Mol Sci. 2023;24(18):14349.
5. Liu XY, Yang LP, Zhao L. Stem cell therapy for Alzheimer's disease. World J Stem Cells. 2020;12(8):787–802.
6. Yi, S., et al., Application of stem cells in peripheral nerve regeneration. Burns & Trauma, 2020. 8: p. tkaa002.

7. Golchin A, et al. Embryonic Stem Cells in Clinical Trials: Current Overview of Developments and Challenges. Adv Exp Med Biol. 2021;1312:19–37.
8. Tada M, et al. Nuclear reprogramming of somatic cells by in vitro hybridization with ES cells. Curr Biol. 2001;11(19):1553–8.
9. Wilmut I, et al. Viable offspring derived from fetal and adult mammalian cells. Cloning Stem Cells. 2007;9(1):3–7.
10. Takahashi K, Yamanaka S. A decade of transcription factor-mediated reprogramming to pluripotency. Nat Rev Mol Cell Biol. 2016;17(3):183–93.
11. Al Abbar A, et al. Induced Pluripotent Stem Cells: Reprogramming Platforms and Applications in Cell Replacement Therapy. Biores Open Access. 2020;9(1):121–36.
12. Kim Y, Jeong J, Choi D. Small-molecule-mediated reprogramming: a silver lining for regenerative medicine. Exp Mol Med. 2020;52(2):213–26.
13. Ye J, et al. Pluripotent stem cells induced from mouse neural stem cells and small intestinal epithelial cells by small molecule compounds. Cell Res. 2016;26(1):34–45.
14. Takashima S, et al. Regulation of pluripotency in male germline stem cells by Dmrt1. Genes Dev. 2013;27(18):1949–58.
15. Liu S, et al. Analysis of chromatin accessibility in p53 deficient spermatogonial stem cells for high frequency transformation into pluripotent state. Cell Prolif. 2022;55(3): e13195.
16. Wei R, et al. A rapid and stable spontaneous reprogramming system of Spermatogonial stem cells to Pluripotent State. Cell Biosci. 2023;13(1):222.
17. Lee Y, et al. Inhibition of Class I Histone Deacetylase Enhances Self-Reprogramming of Spermatogonial Stem Cells into Pluripotent Stem Cells. Int J Stem Cells. 2023;16(1):27–35.
18. Chen Z, et al. Spermatogonial stem cells are a promising and pluripotent cell source for regenerative medicine. Am J Transl Res. 2020;12(11):7048–59.
19. Mizrak SC, et al. Embryonic stem cell-like cells derived from adult human testis. Hum Reprod. 2010;25(1):158–67.
20. Azizi H, et al. Derivation of Pluripotent Cells from Mouse SSCs Seems to Be Age Dependent. Stem Cells Int. 2016;2016:8216312.
21. Ghasemi, N., H. Azizi, and T. Skutella Unraveling the Significance of Nanog in the Generation of Embryonic Stem-like Cells from Spermatogonia Stem Cells: A Combined In Silico Analysis and In Vitro Experimental Approach. International Journal of Molecular Sciences, 2024. 25, https://doi.org/10.3390/ijms25094833.
22. Lin T, et al. p53 induces differentiation of mouse embryonic stem cells by suppressing Nanog expression. Nat Cell Biol. 2005;7(2):165–71.
23. Chen T, et al. Establishment and Maintenance of Genomic Methylation Patterns in Mouse Embryonic Stem Cells by Dnmt3a and Dnmt3b. Mol Cell Biol. 2003;23(16):5594–605.
24. Masaki H, et al. Heterogeneity of pluripotent marker gene expression in colonies generated in human iPS cell induction culture. Stem Cell Research. 2008;1(2):105–15.
25. Wang Y, et al. Lgr4 regulates mammary gland development and stem cell activity through the pluripotency transcription factor Sox2. Stem Cells. 2013;31(9):1921–31.
26. Asadi MH, Javanmardi S, Movahedin M. Derivation of ES-like cell from neonatal mouse testis cells in autologous sertoli cells co-culture system. Iran J Reprod Med. 2014;12(1):37–46.
27. Azizi H, Asgari B, Skutella T. Pluripotency Potential of Embryonic Stem Cell-Like Cells Derived from Mouse Testis. Cell J. 2019;21(3):281–9.
28. Li P, et al. Transcriptional Reactivation of OTX2, RX1 and SIX3 during Reprogramming Contributes to the Generation of RPE Cells from Human iPSCs. Int J Biol Sci. 2016;12(5):505–17.
29. Guo H, et al. Identification of Stemness-Related Genes for Cervical Squamous Cell Carcinoma and Endocervical Adenocarcinoma by Integrated Bioinformatics Analysis. Front Cell Dev Biol. 2021;9: 642724.
30. Kim BN, et al. TGF-β induced EMT and stemness characteristics are associated with epigenetic regulation in lung cancer. Sci Rep. 2020;10(1):10597.
31. Pattabiraman S, et al. Vimentin protects differentiating stem cells from stress. Sci Rep. 2020;10(1):19525.
32. Xu, X., et al., Mouse Dazl and its novel splice variant functions in translational repression of target mRNAs in embryonic stem cells. Biochimica et Biophysica Acta (BBA) - Gene Regulatory Mechanisms, 2013. 1829(5): 425–435.
33. Yu Z, et al. Dazl Promotes Germ Cell Differentiation from Embryonic Stem Cells. J Mol Cell Biol. 2009;1(2):93–103.
34. Chen HH, et al. DAZL limits pluripotency, differentiation, and apoptosis in developing primordial germ cells. Stem Cell Reports. 2014;3(5):892–904.
35. Li Q, et al. Edaravone activates the GDNF/RET neurotrophic signaling pathway and protects mRNA-induced motor neurons from iPS cells. Mol Neurodegener. 2022;17(1):8.
36. Wu X, et al. The POU Domain Transcription Factor POU3F1 Is an Important Intrinsic Regulator of GDNF-Induced Survival and Self-Renewal of Mouse Spermatogonial Stem Cells1. Biol Reprod. 2010;82(6):1103–11.
37. Shamhari, A., et al. The Role of Promyelocytic Leukemia Zinc Finger (PLZF) and Glial-Derived Neurotrophic Factor Family Receptor Alpha 1 (GFRα1) in the Cryopreservation of Spermatogonia Stem Cells. International Journal of Molecular Sciences, 2023. 24, https://doi.org/10.3390/ijms24031945.
38. Zhao H, et al. Wnt signaling in colorectal cancer: pathogenic role and therapeutic target. Mol Cancer. 2022;21(1):144.
39. Sarabia-Sánchez MA, Robles-Flores M. WNT Signaling in Stem Cells: A Look into the Non-Canonical Pathway. Stem Cell Reviews and Reports. 2024;20(1):52–66.
40. Peres de Oliveira, A., et al., Checking NEKs: Overcoming a Bottleneck in Human Diseases. Molecules, 2020. 25(8).
41. Liu L, et al. The cell cycle in stem cell proliferation, pluripotency and differentiation. Nat Cell Biol. 2019;21(9):1060–7.
42. Ramazzotti, G., et al., Phosphoinositide 3 Kinase Signaling in Human Stem Cells from Reprogramming to Differentiation: A Tale in Cytoplasmic and Nuclear Compartments. Int J Mol Sci, 2019. 20(8).
43. Yang J, Jiang W. The Role of SMAD2/3 in Human Embryonic Stem Cells. Front Cell Dev Biol. 2020;8:653.
44. Mossahebi-Mohammadi M, et al. FGF Signaling Pathway: A Key Regulator of Stem Cell Pluripotency. Front Cell Dev Biol. 2020;8:79.
45. Asante, D.M., et al. miR-410 Is a Key Regulator of Epithelial-to-Mesenchymal Transition with Biphasic Role in Prostate Cancer. Cancers, 2024. 16, https://doi.org/10.3390/cancers16010048.
46. Wang C, et al. Biological Functions of Let-7e-5p in Promoting the Differentiation of MC3T3-E1 Cells. Front Cell Dev Biol. 2021;9: 671170.
47. Yuan M, et al. Human umbilical cord mesenchymal stem cells inhibit liver fibrosis via the microRNA-148a-5p/SLIT3 axis. Int Immunopharmacol. 2023;125: 111134.
48. Ding K, et al. MiR-140-5p targets Prox1 to regulate the proliferation and differentiation of neural stem cells through the ERK/MAPK signaling pathway. Ann Transl Med. 2021;9(8):671.
49. Kalaimani L, et al. Hsa-miR-150-5p inhibits Wnt-β-catenin signaling in human corneal epithelial stem cells. Mol Vis. 2022;28:178–91.
50. Lu W, et al. The long non-coding RNA Snhg3 is essential for mouse embryonic stem cell self-renewal and pluripotency. Stem Cell Res Ther. 2019;10(1):157.
51. Amirmahani F, Vallian S, Asadi MH. The LncRNA MIAT is identified as a regulator of stemness-associated transcript in glioma. Mol Biol Rep. 2023;50(1):517–30.
52. Wang J, et al. Long noncoding RNA HOTAIR regulates the stemness of breast cancer cells via activation of the NF-κB signaling pathway. J Biol Chem. 2022;298(12): 102630.

Publisher's Note